

RESEARCH

Open Access



Design, synthesis, and bioactivity of ferulic acid derivatives containing an β -amino alcohol

Ali Dai, Yuanqin Huang, Lijiao Yu, Zhiguo Zheng and Jian Wu*

Abstract

Background: Plant diseases caused by viruses and bacteria cause huge economic losses due to the lack of effective control agents. New potential pesticides can be discovered through biomimetic synthesis and structural modification of natural products. A series of ferulic acid derivatives containing an β -amino alcohol were designed and synthesized, and their biological activities were evaluated.

Result: Bioassays results showed that the EC_{50} values of compound **D24** against *Xanthomonas oryzae* pv. *oryzae* (*Xoo*) was 14.5 μ g/mL, which was better than that of bismethiazol (BT, EC_{50} = 16.2 μ g/mL) and thiodiazole copper (TC, EC_{50} = 44.5 μ g/mL). The in vivo curative and protective activities of compound **D24** against *Xoo* were 50.5% and 50.1%, respectively. The inactivation activities of compounds **D2**, **D3** and **D4** against tobacco mosaic virus (TMV) at 500 μ g/mL were 89.1, 93.7 and 89.5%, respectively, superior to ningnanmycin (93.2%) and ribavirin (73.5%). In particular, the EC_{50} value of compound **D3** was 38.1 μ g/mL, and its molecular docking results showed that compound **D3** had a strong affinity for TMV-CP with a binding energy of -7.54 kcal/mol, which was superior to that of ningnanmycin (-6.88 kcal/mol).

Conclusions: The preliminary mechanism research results indicated that compound **D3** may disrupt the three-dimensional structure of the TMV coat protein, making TMV particles unable to self-assemble, which may provide potential lead compounds for the discovery of novel plant antiviral agents.

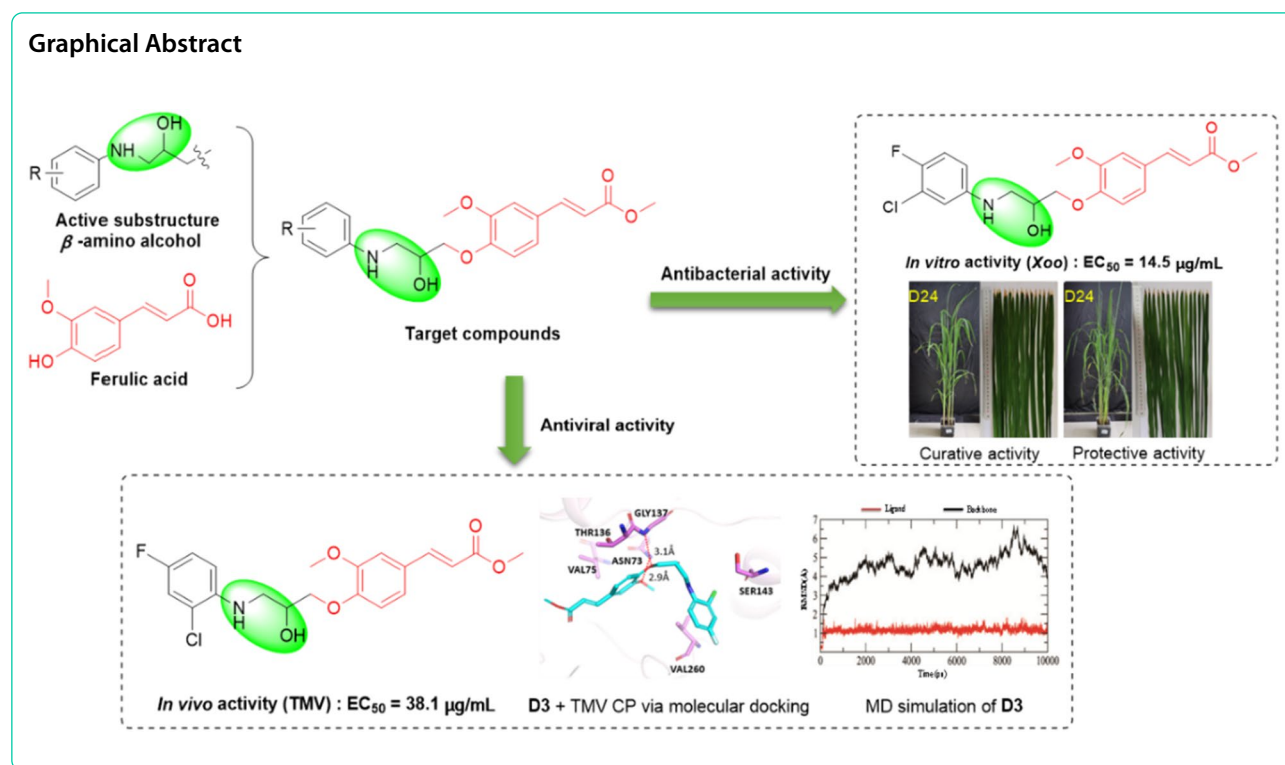
Keywords: Ferulic acid derivatives, β -amino alcohol, Synthesized, Antiviral activity, Antibacterial activity

*Correspondence: jwu6@gzu.edu.cn; wujian2691@126.com

State Key Laboratory Breeding Base of Green Pesticide and Agricultural Bioengineering, Key Laboratory of Green Pesticide and Agricultural Bioengineering, Ministry of Education, Guizhou University, Huaxi District, Guiyang 550025, China



© The Author(s) 2022. **Open Access** This article is licensed under a Creative Commons Attribution 4.0 International License, which permits use, sharing, adaptation, distribution and reproduction in any medium or format, as long as you give appropriate credit to the original author(s) and the source, provide a link to the Creative Commons licence, and indicate if changes were made. The images or other third party material in this article are included in the article's Creative Commons licence, unless indicated otherwise in a credit line to the material. If material is not included in the article's Creative Commons licence and your intended use is not permitted by statutory regulation or exceeds the permitted use, you will need to obtain permission directly from the copyright holder. To view a copy of this licence, visit <http://creativecommons.org/licenses/by/4.0/>. The Creative Commons Public Domain Dedication waiver (<http://creativecommons.org/publicdomain/zero/1.0/>) applies to the data made available in this article, unless otherwise stated in a credit line to the data.



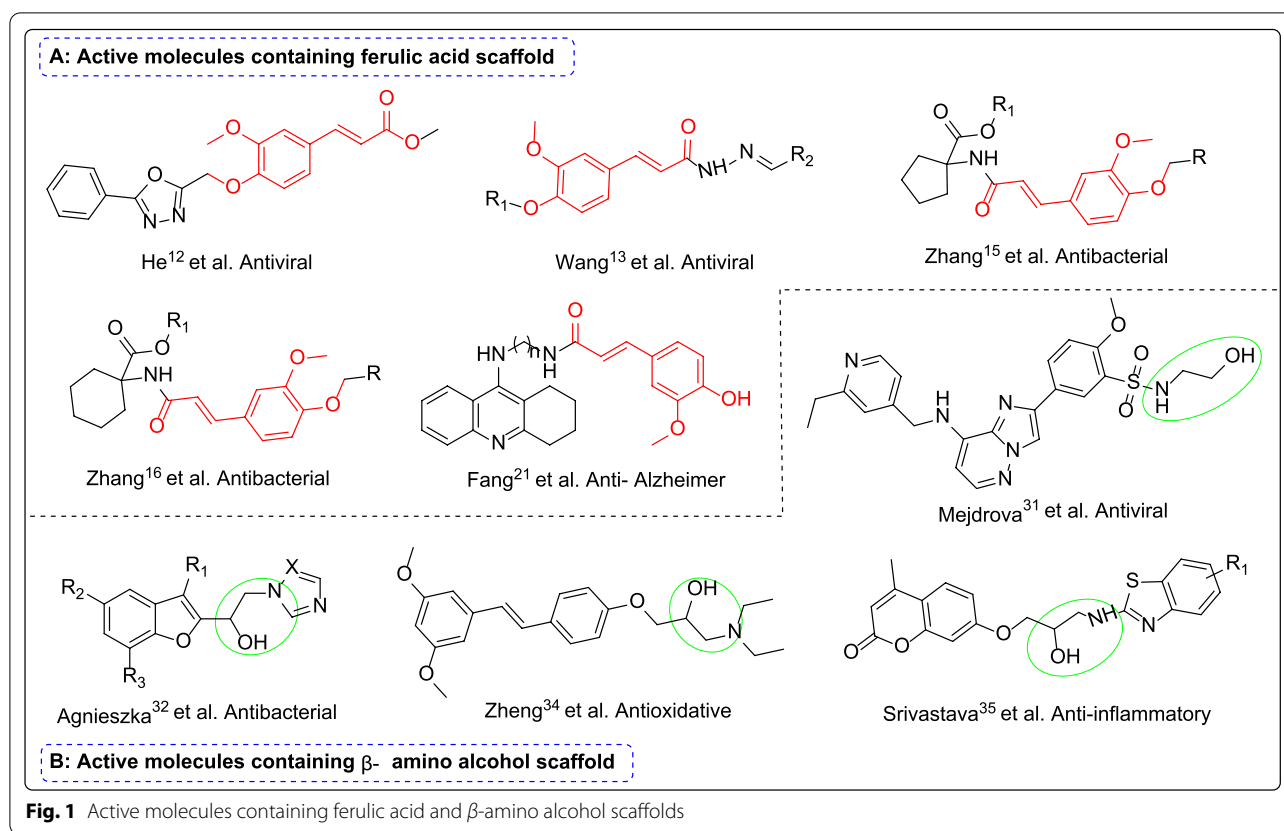
Introduction

Plant pathogens, pests and various abiotic stresses cause serious losses to agricultural production, and are significant problems in achieving agricultural sustainability [1]. So far, more than 1000 plant viruses have been reported [2]. Plant viruses cause huge economic losses to agriculture all over the world every year, amounting to a loss of about \$60 billion (USD) in global annual crop yield [2, 3]. Cucumber mosaic virus (CMV) and tobacco mosaic virus (TMV) are the most common plant viruses. TMV infects crops easily and can overwinter on a variety of plants, and few antiviral drugs can effectively control TMV infection [3, 4]. Plant pathogenic bacteria include *Xanthomonas oryzae* pv. *oryzae* (*Xoo*), which causes rice bacterial blight with crop yield loss of up to 50% [5, 6], and *Xanthomonas axonopodis* pv. *citri* (*Xac*), which causes citrus canker [7]. Extant pesticides for these diseases are ineffective, so new pesticides need to be discovered.

Natural products are a potential alternative for developing new pesticides thanks to their low toxicity to mammals, easy decomposition, environmental friendliness, and unique mode of action [8, 9]. One such product is ferulic acid (FA), the most abundant phenolic acid in the plant. It is cross-linked with polysaccharides and lignin in the structure of the cell wall. It is abundant in *Angelica sinensis*, *Cimicifuga* spp. and *Ligusticum chuanxiong*, and can be isolated from fruits, vegetables, grains, and coffee

beans [2, 4, 10]. Ferulic acid, an α , β -unsaturated carboxylic acid structure, has antiviral properties [11–14]. Some phenolic plant extracts containing ferulic acid can inhibit pathogenic bacteria like *Shigella sonnei*, *Bacillus pneumoniae*, *Escherichia coli*, *Citrobacter*, and *Pseudomonas aeruginosa* [15–19]. In addition, the antioxidant effect of ferulic acid has been verified in several acute and chronic pathologies, such as intestinal ischemia, cardiovascular disease, skin disease, and diabetes [20, 21]. Ferulic acid also has anti-inflammatory [22], anti-cancer activity [23, 24], and is a free radical scavenger and an inhibitor or depolymerizer of amyloid structure [20]. Some of the active compounds containing ferulic acid scaffold are shown in Fig. 1A.

The β -amino alcohol fragment is a common substructure used as a chiral ligand or an auxiliary in asymmetric synthesis, and plays an important role in pharmaceutical chemistry, medicine and organic synthesis [25–28]. A large part of the literature on asymmetric amino hydroxylation focuses on its application in the synthesis of bioactive compounds, many β -amino alcohol derivatives have widely been concerned for their good biological activity [29, 30]. Including antiviral [31], antibacterial [32, 33], antioxidative [34], anti-inflammatory [35], anti-proliferative [36], and anti-cancer [37] properties. Some of the active compounds containing β -amino alcohol scaffold are exemplified in Fig. 1B.



In conclusion, biomimetic synthesis and structural modification of lead compounds of natural products are used to find new pesticides with strong biological activity. In the work described in this paper, ferulic acid derivatives were designed and synthesized in search of highly active compounds, providing potential lead compounds for the discovery of novel plant bactericides and antivirals. Ferulic acid was used as the lead compound, and a β -amino alcohol structure was created by etherifying the phenolic hydroxyl site with an appropriate pesticide molecule. This process synthesized a series of ferulic acid derivatives containing a β -amino alcohol (Fig. 2), and evaluated the antibacterial and antiviral activities of the target compounds.

Experimental Chemistry

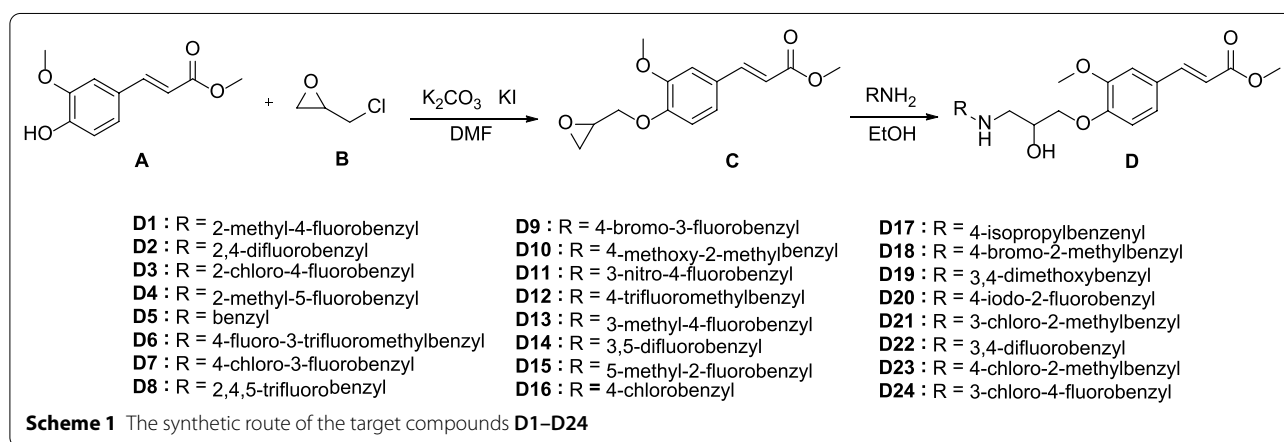
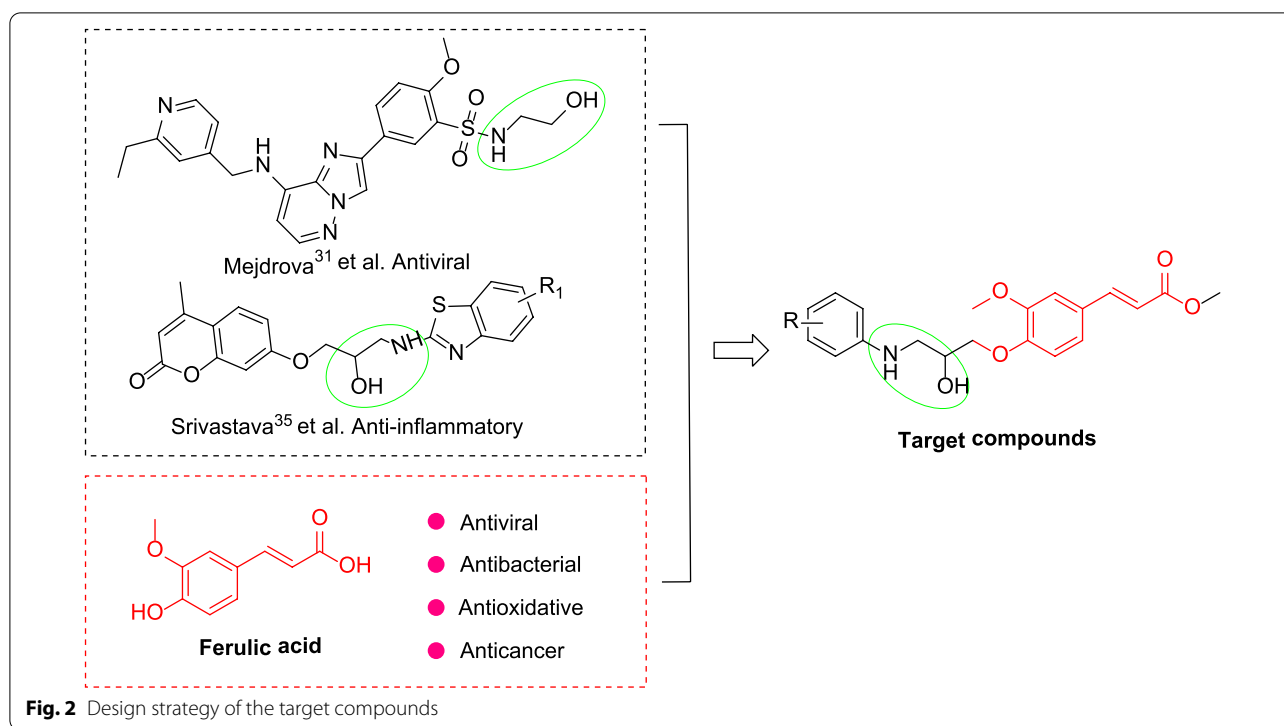
Compounds **D1–D24** can be easily obtained by reported methods [34, 38]. The synthetic route for preparation of the target compounds is depicted in Scheme 1. Under alkaline conditions, methyl ferulate **A** is substituted with epichlorohydrin **B** to obtain intermediate **C**. Then, intermediate **C** undergoes a ring-opening reaction with different substituted amines to obtain target compounds **D1–D24**.

Materials and methods

All reagents and solvents were purchased from commercial companies without further purification and drying. Melting points of synthetic compounds were determined using an XT-4 micro melting point instrument (Beijing Tech Instrument Co., China). All reactions were monitored by thin-layer chromatography (TLC) and identified by UV. The data for ¹H, ¹³C and ¹⁹F NMR of title compounds were obtained with AVANCE III HD 400 MHz (Bruker Corporation, Switzerland) or JEOL-ECX 500 MHz (Japan Electronics Corporation), and used TMS as an internal standard at room temperature. High-resolution mass spectrometer (HR-MS) data was conducted using an Orbitrap LC–MS instrument (Q-Exactive, Thermo Scientific™, USA).

General procedure for the preparation of intermediate C

Methyl (*E*)-3-(4-hydroxy-3-methoxyphenyl)acrylate (**A**) (2.00 g, 1 mmol), anhydrous K₂CO₃ (1.59 g, 1.2 mmol) and KI (0.79 g, 0.5 mmol) were dissolved in DMF and stirred at room temperature for 2–3 h. Then to this solution was added epichlorohydrin (**B**) (1.07 g, 1.2 mmol) and refluxed for 5–6 h. After completion of the reaction, the resulted mixture was diluted with water and



extracted with ethyl acetate, the organic layer was dried over by NaSO_4 and concentrated under vacuum. The residue was purified by silica gel chromatography with petroleum ether/ethyl acetate (8:1), concentrated eluent to give solid intermediate **C**.

General procedure for the preparation of target compounds **D1–D24**

Methyl (*E*)-3-(3-methoxy-4-(oxiran-2-ylmethoxy)phenyl)acrylate (**C**) (150.00 mg, 1 mmol) and various substituted aniline (284.13 mg, 4 mmol) were dissolved in ethanol (6 mL) and refluxed for 6–8 h. Upon completion of the

reaction, and an appropriate amount of water was added to the system to get white solid, the precipitate was collected by filtration. Then crude compound was subjected to column chromatography with petroleum ether/ethyl acetate (3:1) to afford target compounds **D1–D24**. Their structures were identified by ^1H NMR, ^{13}C NMR, ^{19}F NMR, and HR-MS.

Methyl(E)-3-(4-(3-((4-fluoro-2-methylphenyl)amino)-2-hydroxypropoxy)-3-methoxyphenyl)acrylate (D1)

Yield 83%; Purple solid; m.p. 66–68 °C. ^1H NMR (400 MHz, CDCl_3) δ 7.63 (d, $J = 15.9$ Hz, 1H), 7.13–7.04

(m, 2H), 6.89 (d, $J=8.3$ Hz, 1H), 6.85–6.76 (m, 2H), 6.59–6.54 (m, 1H), 6.33 (d, $J=15.9$ Hz, 1H), 4.37–4.27 (m, 1H), 4.14 (ddd, $J=16.2, 9.7, 5.1$ Hz, 2H), 3.89 (s, 3H), 3.80 (s, 3H), 3.35 (ddd, $J=19.3, 12.5, 5.6$ Hz, 2H), 2.16 (s, 3H). ^{13}C NMR (100 MHz, CDCl_3) δ 167.6, 155.7 (d, $J=235.1$ Hz), 149.9, 149.6, 144.5, 142.2, 128.3, 124.7 (d, $J=7.2$ Hz), 122.4, 117.0 (d, $J=22.4$ Hz), 116.0, 113.7, 112.7 (d, $J=21.6$ Hz), 110.9 (d, $J=7.8$ Hz), 110.1, 72.2, 68.4, 55.8, 51.7, 47.0, 17.5. ^{19}F NMR (376 MHz, CDCl_3) δ –127.92. HRMS (ESI+) m/z Calcd for $\text{C}_{21}\text{H}_{25}\text{FNO}_5$ $[\text{M}+\text{H}]^+$ 390.17113; Found 390.17090.

Methyl(E)-3-(4-(3-((2,4-difluorophenyl)amino)-2-hydroxypropoxy)-3-methoxyphenyl)acrylate (D2)

Yield 80%; White solid; m.p. 69–71 °C. ^1H NMR (400 MHz, CDCl_3) δ 7.63 (d, $J=15.9$ Hz, 1H), 7.14–7.01 (m, 2H), 6.88 (d, $J=8.2$ Hz, 1H), 6.83–6.64 (m, 3H), 6.32 (d, $J=15.9$ Hz, 1H), 4.33–4.26 (m, 1H), 4.13 (ddd, $J=16.0, 9.7, 5.0$ Hz, 2H), 3.89 (s, 3H), 3.80 (s, 3H), 3.37 (ddd, $J=19.2, 12.8, 5.5$ Hz, 2H). ^{13}C NMR (100 MHz, CDCl_3) δ 167.6, 154.5 (dd, $J=238.1, 11.1$ Hz), 151.2 (dd, $J=242.3, 11.7$ Hz), 149.9, 149.6, 144.5, 133.1 (dd, $J=11.7, 2.9$ Hz), 128.3, 122.3, 116.0, 113.6, 112.5 (dd, $J=8.8, 4.4$ Hz), 110.6 (dd, $J=21.6, 3.8$ Hz), 110.1, 103.5 (dd, $J=26.6, 22.8$ Hz), 72.0, 68.4, 55.7, 51.7, 46.6. ^{19}F NMR (376 MHz, CDCl_3) δ –125.26, –131.24. HRMS (ESI+) m/z Calcd for $\text{C}_{20}\text{H}_{22}\text{F}_2\text{NO}_5$ $[\text{M}+\text{H}]^+$ 394.14606; Found 394.14606.

Methyl(E)-3-(4-(3-((2-chloro-4-fluorophenyl)amino)-2-hydroxypropoxy)-3-methoxyphenyl)acrylate (D3)

Yield 83%; White solid; m.p. 71–73 °C. ^1H NMR (400 MHz, CDCl_3) δ 7.63 (d, $J=16.0$ Hz, 1H), 7.14–7.03 (m, 3H), 6.93–6.84 (m, 2H), 6.66 (dd, $J=9.0, 5.0$ Hz, 1H), 6.33 (d, $J=15.9$ Hz, 1H), 4.30 (dq, $J=6.6, 4.4$ Hz, 1H), 4.13 (qd, $J=9.7, 5.1$ Hz, 2H), 3.89 (s, 3H), 3.80 (s, 3H), 3.38 (ddd, $J=19.6, 12.8, 5.7$ Hz, 2H). ^{13}C NMR (100 MHz, CDCl_3) δ 167.6, 154.6 (d, $J=238.4$ Hz), 149.9, 149.6, 144.5, 140.7 (d, $J=2.3$ Hz), 128.4, 122.4, 119.5 (d, $J=10.2$ Hz), 116.6, 116.4, 116.0, 114.4, 114.2, 113.8, 111.7 (d, $J=8.0$ Hz), 71.8, 68.4, 55.8, 51.7, 46.5. ^{19}F NMR (376 MHz, CDCl_3) δ –126.52. HRMS (ESI+) m/z Calcd for $\text{C}_{20}\text{H}_{22}\text{FCINO}_5$ $[\text{M}+\text{H}]^+$ 410.11651; Found 410.11646.

Methyl(E)-3-(4-(3-((5-fluoro-2-methylphenyl)amino)-2-hydroxypropoxy)-3-methoxyphenyl)acrylate (D4)

Yield 60%; White solid; m.p. 104–105 °C. ^1H NMR (400 MHz, CDCl_3) δ 7.63 (d, $J=16.0$ Hz, 1H), 7.11–7.04 (m, 2H), 6.96 (t, $J=7.5$ Hz, 1H), 6.89 (d, $J=8.2$ Hz, 1H), 6.39–6.30 (m, 3H), 4.32 (ddd, $J=10.3, 6.5, 4.0$ Hz, 1H), 4.13 (ddd, $J=16.1, 9.7, 5.1$ Hz, 2H), 3.89 (s, 3H), 3.80 (s, 3H), 3.36 (ddd, $J=19.6, 12.8, 5.6$ Hz, 2H), 2.10 (s, 3H). ^{13}C

NMR (100 MHz, CDCl_3) δ 167.5, 162.7 (d, $J=240.3$ Hz), 149.9, 149.7, 147.3 (d, $J=10.4$ Hz), 144.5, 130.6 (d, $J=9.8$ Hz), 128.4, 122.3, 117.9 (d, $J=2.7$ Hz), 116.0, 113.8, 110.1, 103.1 (d, $J=21.1$ Hz), 97.5 (d, $J=26.2$ Hz), 72.0, 68.3, 55.7, 51.7, 46.2, 16.8. ^{19}F NMR (376 MHz, CDCl_3) δ –115.66. HRMS (ESI+) m/z Calcd for $\text{C}_{21}\text{H}_{25}\text{FNO}_5$ $[\text{M}+\text{H}]^+$ 390.17113; Found 390.17099.

Methyl(E)-3-(4-(2-hydroxy-3-(phenylamino)propoxy)-3-methoxyphenyl)acrylate (D5)

Yield 70%; White solid; m.p. 94–95 °C. ^1H NMR (400 MHz, CDCl_3) δ 7.63 (d, $J=15.9$ Hz, 1H), 7.19 (dd, $J=8.4, 7.4$ Hz, 2H), 7.09–7.04 (m, 2H), 6.87 (d, $J=8.2$ Hz, 1H), 6.74 (t, $J=7.3$ Hz, 1H), 6.69 (s, 1H), 6.67 (s, 1H), 6.32 (d, $J=15.9$ Hz, 1H), 4.31–4.26 (m, 1H), 4.13 (ddd, $J=16.0, 9.7, 5.0$ Hz, 2H), 3.89 (s, 3H), 3.80 (s, 3H), 3.38 (ddd, $J=19.2, 12.9, 5.5$ Hz, 2H). ^{13}C NMR (100 MHz, CDCl_3) δ 167.6, 150.0, 149.6, 148.0, 144.6, 129.3, 128.3, 122.4, 118.1, 115.9, 113.6, 113.3, 110.1, 72.1, 68.4, 55.8, 51.7, 46.6. HRMS (ESI+) m/z Calcd for $\text{C}_{20}\text{H}_{24}\text{NO}_5$ $[\text{M}+\text{H}]^+$ 358.16490; Found 358.16492.

Methyl(E)-3-(4-(3-((4-fluoro-3-(trifluoromethyl)phenyl)amino)-2-hydroxypropoxy)-3-methoxyphenyl)acrylate (D6)

Yield 88%; White solid; m.p. 112–114 °C. ^1H NMR (400 MHz, CDCl_3) δ 7.63 (d, $J=16.0$ Hz, 1H), 7.13–6.97 (m, 3H), 6.91–6.72 (m, 3H), 6.33 (d, $J=15.9$ Hz, 1H), 4.32–4.24 (m, 1H), 4.20–4.07 (m, 2H), 3.90 (s, 3H), 3.80 (s, 3H), 3.45–3.23 (m, 2H). ^{13}C NMR (100 MHz, CDCl_3) δ 167.6, 152.3 (d, $J=245.3$ Hz), 149.7, 149.5, 144.4, 144.4 (d, $J=2.1$ Hz), 128.4, 122.7 (q, $J=273.5$ Hz), 122.4, 117.6, 117.4, 117.4, 116.1, 113.5, 110.5 (d, $J=4.5$ Hz), 110.1, 72.1, 68.2, 55.8, 51.7, 46.9. ^{19}F NMR (376 MHz, CDCl_3) δ –61.47, –130.02. HRMS (ESI+) m/z Calcd for $\text{C}_{21}\text{H}_{22}\text{F}_4\text{NO}_5$ $[\text{M}+\text{H}]^+$ 444.14286; Found 444.14114.

Methyl(E)-3-(4-(3-((4-chloro-3-fluorophenyl)amino)-2-hydroxypropoxy)-3-methoxyphenyl)acrylate (D7)

Yield 89%; White solid; m.p. 124–126 °C. ^1H NMR (400 MHz, CDCl_3) δ 7.63 (d, $J=16.0$ Hz, 1H), 7.15–7.03 (m, 3H), 6.87 (d, $J=8.2$ Hz, 1H), 6.46–6.35 (m, 2H), 6.33 (d, $J=15.9$ Hz, 1H), 4.29–4.22 (m, 1H), 4.11 (ddd, $J=15.8, 9.6, 5.0$ Hz, 2H), 3.90 (s, 3H), 3.80 (s, 3H), 3.32 (ddd, $J=19.3, 12.8, 5.4$ Hz, 2H). ^{13}C NMR (100 MHz, CDCl_3) δ 167.6, 158.8 (d, $J=245.5$ Hz), 149.7, 149.6, 148.5 (d, $J=9.7$ Hz), 144.5, 130.6 (d, $J=1.3$ Hz), 128.4, 122.4, 116.1, 113.6, 110.1, 109.8 (d, $J=2.8$ Hz), 108.3 (d, $J=18.1$ Hz), 101.0, 100.7, 72.0, 68.2, 55.8, 51.7, 46.4. ^{19}F NMR (376 MHz, CDCl_3) δ –115.00. HRMS (ESI+) m/z Calcd for $\text{C}_{20}\text{H}_{20}\text{FCINO}_5$ $[\text{M}+\text{H}]^+$ 408.10086; Found 408.10153.

Methyl(E)-3-(4-(2-hydroxy-3-((2,4,5-trifluorophenyl)amino)propoxy)-3-methoxyphenyl)acrylate (D8)

Yield 87%; White solid; m.p. 112–114 °C. ^1H NMR (400 MHz, CDCl_3) δ 7.63 (d, $J=15.9$ Hz, 1H), 7.11–7.03 (m, 2H), 6.92–6.82 (m, 2H), 6.58 (dt, $J=12.2$, 7.9 Hz, 1H), 6.33 (d, $J=15.9$ Hz, 1H), 4.37 (s, 1H, OH), 4.27 (d, $J=4.1$ Hz, 1H), 4.12 (ddd, $J=15.7$, 9.6, 5.0 Hz, 2H), 3.90 (s, 3H), 3.80 (s, 3H), 3.45–3.23 (m, 2H). ^{13}C NMR (100 MHz, CDCl_3) δ 167.7, 149.8, 149.6, 147.0 (ddd, $J=15.4$, 13.0, 3.2 Hz), 146.3 (ddd, $J=12.6$, 10.0, 7.56 Hz), 144.6, 140.8 (ddd, $J=26.0$, 13.9, 11.4 Hz), 133.5, 128.5, 122.4, 116.1, 113.6, 110.2, 104.8 (t, $J=23.3$ Hz), 100.8 (dd, $J=23.6$, 4.0 Hz), 71.7, 68.4, 55.8, 51.7, 46.5. ^{19}F NMR (376 MHz, CDCl_3) δ –137.98, –142.42, –150.59. HRMS (ESI+) m/z Calcd for $\text{C}_{20}\text{H}_{20}\text{F}_3\text{NO}_5\text{K}$ $[\text{M}+\text{K}]^+$ 450.09252; Found 450.09174.

Methyl(E)-3-(4-(3-((4-bromo-3-fluorophenyl)amino)-2-hydroxypropoxy)-3-methoxyphenyl)acrylate (D9)

Yield 75%; Yellow solid; m.p. 125–127 °C. ^1H NMR (500 MHz, CDCl_3) δ 7.61 (d, $J=15.9$ Hz, 1H), 7.22 (d, $J=8.3$ Hz, 1H), 7.10–7.01 (m, 2H), 6.85 (d, $J=8.3$ Hz, 1H), 6.41 (dd, $J=11.1$, 2.6 Hz, 1H), 6.34–6.27 (m, 2H), 4.24 (ddd, $J=10.3$, 6.2, 4.3 Hz, 1H), 4.15–4.03 (m, 2H), 3.88 (s, 3H), 3.79 (s, 3H), 3.41–3.19 (m, 2H). ^{13}C NMR (125 MHz, CDCl_3) δ 167.6, 159.9 (d, $J=244.1$ Hz), 149.8, 149.7, 149.3 (d, $J=9.8$ Hz), 144.5, 133.4, 128.5, 122.5, 116.2, 113.7, 110.5 (d, $J=1.8$ Hz), 110.2, 100.9 (d, $J=26.2$ Hz), 95.2 (d, $J=21.1$ Hz), 72.1, 68.3, 55.9, 51.8, 46.4. ^{19}F NMR (376 MHz, CDCl_3) δ –107.03. HRMS (ESI+) m/z Calcd for $\text{C}_{20}\text{H}_{22}\text{FBrNO}_5$ $[\text{M}+\text{H}]^+$ 454.06599; Found 454.06580.

Methyl(E)-3-(4-(2-hydroxy-3-((4-methoxy-2-methylphenyl)amino)propoxy)-3-methoxyphenyl)acrylate (D10)

Yield 95%; Purple solid; m.p. 64–66 °C. ^1H NMR (400 MHz, CDCl_3) δ 7.63 (d, $J=15.9$ Hz, 1H), 7.11–7.04 (m, 2H), 6.89 (d, $J=8.3$ Hz, 1H), 6.72–6.67 (m, 2H), 6.61 (d, $J=8.5$ Hz, 1H), 6.32 (d, $J=15.9$ Hz, 1H), 4.32 (ddd, $J=10.6$, 6.8, 4.1 Hz, 1H), 4.13 (ddd, $J=16.2$, 9.7, 5.1 Hz, 2H), 3.88 (s, 3H), 3.80 (s, 3H), 3.74 (s, 3H), 3.34 (ddd, $J=19.3$, 12.6, 5.6 Hz, 2H), 2.17 (s, 3H). ^{13}C NMR (100 MHz, CDCl_3) δ 167.6, 152.1, 150.0, 149.6, 144.6, 140.1, 128.2, 124.9, 122.4, 116.9, 115.9, 113.5, 111.6, 111.5, 110.1, 72.2, 68.4, 55.8, 55.7, 51.6, 47.3, 17.7. HRMS (ESI+) m/z Calcd for $\text{C}_{22}\text{H}_{28}\text{NO}_6$ $[\text{M}+\text{H}]^+$ 402.19111; Found 402.18994.

Methyl(E)-3-(4-(3-((4-fluoro-3-nitrophenyl)amino)-2-hydroxypropoxy)-3-methoxyphenyl)acrylate (D11)

Yield 75%; Yellow solid; m.p. 136–138 °C. ^1H NMR (400 MHz, CDCl_3) δ 7.63 (d, $J=15.9$ Hz, 1H), 7.26–7.23

(m, 1H), 7.11 (d, $J=2.2$ Hz, 1H), 7.09 (d, $J=1.4$ Hz, 1H), 7.07 (d, $J=1.7$ Hz, 1H), 6.90 (d, $J=5.1$ Hz, 1H), 6.89–6.85 (m, 1H), 6.34 (d, $J=15.9$ Hz, 1H), 4.33–4.27 (m, 1H), 4.22–4.08 (m, 2H), 3.93 (s, 3H), 3.81 (s, 3H), 3.46 (dd, $J=12.5$, 4.3 Hz, 1H), 3.31 (dd, $J=12.5$, 6.2 Hz, 1H). ^{13}C NMR (100 MHz, CDCl_3) δ 167.5, 149.7, 149.6, 148.2 (d, $J=254.9$ Hz), 14.82 (d, $J=2.3$ Hz), 144.4, 137.4, 128.7, 122.3, 119.9 (d, $J=7.1$ Hz), 118.9 (d, $J=22.3$ Hz), 116.2, 113.8, 110.2, 108.0 (d, $J=3.1$ Hz), 72.2, 68.1, 55.8, 51.7, 46.7. ^{19}F NMR (376 MHz, CDCl_3) δ –132.70. HRMS (ESI+) m/z Calcd for $\text{C}_{20}\text{H}_{22}\text{FN}_2\text{O}_7$ $[\text{M}+\text{H}]^+$ 421.14056; Found 421.14011.

Methyl(E)-3-(4-(2-hydroxy-3-((4-(trifluoromethyl)phenyl)amino)propoxy)-3-methoxyphenyl)acrylate (D12)

Yield 75%; Yellow solid; m.p. 98–100 °C. ^1H NMR (500 MHz, CDCl_3) δ 7.61 (d, $J=15.9$ Hz, 1H), 7.38 (d, $J=8.5$ Hz, 2H), 7.09–7.01 (m, 2H), 6.85 (d, $J=8.2$ Hz, 1H), 6.64 (d, $J=8.5$ Hz, 2H), 6.31 (d, $J=16.0$ Hz, 1H), 4.26 (dq, $J=6.3$, 4.4 Hz, 1H), 4.10 (ddd, $J=15.8$, 9.6, 5.0 Hz, 2H), 3.87 (s, 3H), 3.78 (s, 3H), 3.49–3.27 (m, 2H). ^{13}C NMR (125 MHz, CDCl_3) δ 167.6, 150.7, 149.9, 149.6, 144.5, 128.5, 126.7, 126.7, 124.9 (q, $J=270.2$ Hz), 122.5, 119.4, 119.1, 116.2, 113.7, 112.3, 110.2, 72.1, 68.4, 55.9, 51.8, 46.0. ^{19}F NMR (376 MHz, CDCl_3) δ –60.91. HRMS (ESI+) m/z Calcd for $\text{C}_{21}\text{H}_{23}\text{F}_3\text{NO}_5$ $[\text{M}+\text{H}]^+$ 426.15228; Found 426.15213.

Methyl(E)-3-(4-(3-((4-fluoro-3-methylphenyl)amino)-2-hydroxypropoxy)-3-methoxyphenyl)acrylate (D13)

Yield 92%; White solid; m.p. 121–123 °C. ^1H NMR (400 MHz, CDCl_3) δ 7.63 (d, $J=15.8$ Hz, 1H), 7.15–7.02 (m, 2H), 6.93–6.79 (m, 2H), 6.47 (d, $J=14.9$ Hz, 2H), 6.32 (d, $J=16.0$ Hz, 1H), 4.27 (s, 1H), 4.19–4.05 (m, 2H), 3.90 (s, 3H), 3.80 (s, 3H), 3.43–3.21 (m, 2H), 2.20 (s, 3H). ^{13}C NMR (100 MHz, CDCl_3) δ 167.6, 154.8 (d, $J=234.8$ Hz), 149.9, 149.6, 144.5, 144.1, 128.3, 125.3 (d, $J=18.2$ Hz), 122.4, δ 116.0 (d, $J=7.7$ Hz), 115.4, 115.2, 113.6, 111.7 (d, $J=7.5$ Hz), 110.1, 72.1, 68.4, 55.8, 51.7, 47.3, 14.8. ^{19}F NMR (376 MHz, CDCl_3) δ –131.50. HRMS (ESI+) m/z Calcd for $\text{C}_{21}\text{H}_{25}\text{FNO}_5$ $[\text{M}+\text{H}]^+$ 390.17113; Found 390.16953.

Methyl(E)-3-(4-(3-((3,5-difluorophenyl)amino)-2-hydroxypropoxy)-3-methoxyphenyl)acrylate (D14)

Yield 93%; White solid; m.p. 107–109 °C. ^1H NMR (400 MHz, CDCl_3) δ 7.63 (d, $J=16.0$ Hz, 1H), 7.15–7.02 (m, 2H), 6.87 (d, $J=8.2$ Hz, 1H), 6.33 (d, $J=15.9$ Hz, 1H), 6.20–6.10 (m, 3H), 4.59 (s, 1H, OH), 4.33–4.22 (m, 1H), 4.10 (ddd, $J=15.8$, 9.6, 4.9 Hz, 2H), 3.90 (s, 3H), 3.80

(s, 3H), 3.33 (ddd, $J=19.3, 12.8, 5.1$ Hz, 2H). ^{13}C NMR (100 MHz, CDCl_3) δ 167.6, 164.2 (d, $J=244.1$ Hz), 164.0 (d, $J=244.1$ Hz), 150.4 (d, $J=26.5$ Hz), 149.7, 149.5, 144.5, 128.4, 122.4, 116.1, 113.5, 110.1, 95.7 (d, $J=28.6$ Hz), 92.8 (d, $J=26.2$ Hz), 92.4, 71.9, 68.2, 55.8, 51.7, 46.2. ^{19}F NMR (376 MHz, CDCl_3) δ -110.28. HRMS (ESI+) m/z Calcd for $\text{C}_{20}\text{H}_{20}\text{F}_2\text{NO}_5$ $[\text{M}-\text{H}]^-$ 392.13041; Found 392.13141.

Methyl(E)-3-(4-(3-((2-fluoro-5-methylphenyl)amino)-2-hydroxypropoxy)-3-methoxyphenyl)acrylate (D15)

Yield 92%; White solid; m.p. 95–97 °C. ^1H NMR (400 MHz, CDCl_3) δ 7.62 (d, $J=15.9$ Hz, 1H), 7.09–7.01 (m, 2H), 6.90–6.80 (m, 2H), 6.55 (dd, $J=8.4, 1.6$ Hz, 1H), 6.47–6.40 (m, 1H), 6.31 (d, $J=15.9$ Hz, 1H), 4.35–4.24 (m, 1H), 4.11 (ddd, $J=15.8, 9.7, 5.0$ Hz, 2H), 3.88 (s, 3H), 3.80 (s, 3H), 3.39 (ddd, $J=19.4, 13.0, 5.6$ Hz, 2H), 2.23 (s, 3H). ^{13}C NMR (100 MHz, CDCl_3) δ 167.6, 150.1 (d, $J=236.2$ Hz), 149.9, 149.6, 144.6, 136.0 (d, $J=11.7$ Hz), 134.0 (d, $J=3.4$ Hz), 128.2, 122.4, 117.4 (d, $J=6.8$ Hz), 115.9, 114.1 (d, $J=18.5$ Hz), 113.4, 113.1 (d, $J=2.9$ Hz), 110.1, 71.7, 68.4, 55.7, 51.6, 46.1, 21.1. ^{19}F NMR (376 MHz, CDCl_3) δ -140.64. HRMS (ESI+) m/z Calcd for $\text{C}_{21}\text{H}_{24}\text{FNO}_5\text{K}$ $[\text{M}+\text{K}]^+$ 428.12701; Found 428.12668.

Methyl(E)-3-(4-(3-((4-chlorophenyl)amino)-2-hydroxypropoxy)-3-methoxyphenyl)acrylate (D16)

Yield 90%; White solid; m.p. 98–100 °C. ^1H NMR (500 MHz, CDCl_3) δ 7.61 (d, $J=15.9$ Hz, 1H), 7.04 (m, $J=4.2, 1.7$ Hz, 3H), 6.84 (d, $J=8.3$ Hz, 1H), 6.64 (ddd, $J=20.5, 5.7, 1.6$ Hz, 2H), 6.55–6.47 (m, 1H), 6.30 (d, $J=15.9$ Hz, 1H), 4.25 (dq, $J=6.2, 4.4$ Hz, 1H), 4.09 (ddd, $J=15.8, 9.6, 5.0$ Hz, 2H), 3.87 (s, 3H), 3.78 (s, 3H), 3.33 (ddd, $J=19.3, 12.8, 5.5$ Hz, 2H). ^{13}C NMR (125 MHz, CDCl_3) δ 167.7, 149.9, 149.6, 149.4, 144.6, 135.1, 130.3, 128.4, 122.5, 117.7, 116.1, 113.6, 112.8, 111.6, 110.2, 72.1, 68.3, 55.9, 51.8, 46.4. HRMS (ESI+) m/z Calcd for $\text{C}_{20}\text{H}_{23}\text{ClNO}_5$ $[\text{M}+\text{H}]^+$ 392.12593; Found 392.12589.

Methyl(E)-3-(4-(2-hydroxy-3-((4-isopropylphenyl)amino)propoxy)-3-methoxyphenyl)acrylate (D17)

Yield 82%; White solid; m.p. 84–86 °C. ^1H NMR (400 MHz, CDCl_3) δ 7.62 (d, $J=15.9$ Hz, 1H), 7.15–6.98 (m, 3H), 6.87 (d, $J=8.2$ Hz, 1H), 6.63 (d, $J=7.6$ Hz, 1H), 6.55 (s, 1H), 6.50 (dd, $J=7.9, 1.7$ Hz, 1H), 6.32 (d, $J=15.9$ Hz, 1H), 4.28 (dt, $J=6.2, 5.4$ Hz, 1H), 4.12 (ddd, $J=15.9, 9.7, 5.0$ Hz, 2H), 3.88 (s, 3H), 3.80 (s, 3H), 3.38 (ddd, $J=19.2, 12.8, 5.5$ Hz, 2H), 2.80 (dt, $J=13.8, 6.9$ Hz, 1H), 1.22 (s, 3H), 1.21 (s, 3H). ^{13}C NMR (100 MHz, CDCl_3) δ 167.6, 150.2, 149.5, 148.1, 144.61, 129.2, 128.1, 122.4, 116.3, 115.9, 113.4, 111.7, 110.7, 110.1, 72.0, 68.4, 55.8, 51.6, 46.6, 34.2, 23.9. HRMS (ESI+) m/z Calcd for $\text{C}_{23}\text{H}_{30}\text{NO}_5$ $[\text{M}+\text{H}]^+$ 400.21185; Found 400.21164.

Methyl(E)-3-(4-(3-((4-bromo-2-methylphenyl)amino)-2-hydroxypropoxy)-3-methoxyphenyl)acrylate (D18)

Yield 83%; White solid; m.p. 100–101 °C. ^1H NMR (400 MHz, CDCl_3) δ 7.62 (d, $J=15.9$ Hz, 1H), 7.22–7.14 (m, 2H), 7.11–7.02 (m, 2H), 6.87 (d, $J=8.2$ Hz, 1H), 6.51 (d, $J=8.5$ Hz, 1H), 6.32 (d, $J=15.9$ Hz, 1H), 4.37–4.26 (m, 1H), 4.11 (ddd, $J=16.1, 9.7, 5.1$ Hz, 2H), 3.87 (s, 3H), 3.80 (s, 3H), 3.35 (ddd, $J=19.5, 12.7, 5.6$ Hz, 2H), 2.12 (s, 3H). ^{13}C NMR (100 MHz, CDCl_3) δ 167.6, 149.9, 149.6, 145.1, 144.5, 132.6, 129.6, 128.4, 124.9, 122.4, 116.0, 113.7, 111.5, 110.2, 109.2, 72.1, 68.4, 55.8, 51.7, 46.4, 17.2. HRMS (ESI+) m/z Calcd for $\text{C}_{21}\text{H}_{25}\text{BrNO}_5$ $[\text{M}+\text{H}]^+$ 450.09106; Found 450.09048.

Methyl(E)-3-(4-(3-((3,4-dimethoxyphenyl)amino)-2-hydroxypropoxy)-3-methoxyphenyl)acrylate (D19)

Yield 90%; Gray solid; m.p. 101–103 °C. ^1H NMR (400 MHz, CDCl_3) δ 7.63 (d, $J=15.9$ Hz, 1H), 7.11–7.04 (m, 2H), 6.88 (d, $J=8.3$ Hz, 1H), 6.75 (d, $J=8.6$ Hz, 1H), 6.32 (dd, $J=9.2, 6.7$ Hz, 2H), 6.22 (dd, $J=8.5, 2.6$ Hz, 1H), 4.31–4.26 (m, 1H), 4.13 (ddd, $J=16.0, 9.7, 5.0$ Hz, 2H), 3.89 (s, 3H), 3.83 (s, 3H), 3.81 (s, 3H), 3.80 (s, 3H), 3.34 (ddd, $J=19.1, 12.6, 5.4$ Hz, 2H). ^{13}C NMR (100 MHz, CDCl_3) δ 167.6, 150.0, 149.9, 149.6, 144.5, 142.8, 142.0, 128.2, 122.4, 116.0, 113.5, 112.9, 110.1, 104.1, 99.5, 72.1, 68.4, 56.6, 55.8, 55.7, 51.7, 47.5. HRMS (ESI+) m/z Calcd for $\text{C}_{22}\text{H}_{27}\text{NO}_7$ $[\text{M}+\text{H}]^+$ 418.18603; Found 418.18582.

Methyl(E)-3-(4-(3-((2-fluoro-4-iodophenyl)amino)-2-hydroxypropoxy)-3-methoxyphenyl)acrylate (D20)

Yield 84%; White solid; m.p. 105–107 °C. ^1H NMR (400 MHz, CDCl_3) δ 7.62 (d, $J=15.9$ Hz, 1H), 7.30–7.21 (m, 2H), 7.10–7.01 (m, 2H), 6.86 (d, $J=8.2$ Hz, 1H), 6.50 (t, $J=8.8$ Hz, 1H), 6.32 (d, $J=15.9$ Hz, 1H), 4.34–4.04 (m, 1H), δ 4.10 (ddd, $J=15.7, 9.6, 4.9$ Hz, 2H) 0.388 (s, 3H), 3.80 (s, 3H), 3.36 (ddd, $J=19.3, 13.0, 5.4$ Hz, 2H). ^{13}C NMR (100 MHz, CDCl_3) δ 167.6, 151.5 (d, $J=244.5$ Hz), 149.8, 149.6, 144.5, 136.6 (d, $J=11.4$ Hz), 133.4 (d, $J=3.6$ Hz), 128.4, 123.4, 123.2, 122.4, 116.0, 113.9 (d, $J=3.5$ Hz), 113.6, 110.1, 71.8, 68.3, 55.8, 51.7, 45.9. ^{19}F NMR (376 MHz, CDCl_3) δ -133.02. HRMS (ESI+) m/z Calcd for $\text{C}_{20}\text{H}_{22}\text{FINO}_5$ $[\text{M}+\text{H}]^+$ 502.05212; Found 502.05151.

Methyl(E)-3-(4-(3-((3-chloro-2-methylphenyl)amino)-2-hydroxypropoxy)-3-methoxyphenyl)acrylate (D21)

Yield 92%; Pink solid; m.p. 77–78 °C. ^1H NMR (400 MHz, CDCl_3) δ 7.63 (d, $J=16.0$ Hz, 1H), 7.12–6.98 (m, 3H), 6.88 (d, $J=8.3$ Hz, 1H), 6.79 (d, $J=7.5$ Hz, 1H), 6.55 (d, $J=8.0$ Hz, 1H), 6.32 (d, $J=15.9$ Hz, 1H), 4.33 (s, 1H, OH),

4.13 (ddd, $J=16.2, 9.7, 5.1$ Hz, 3H, CH₂, CH), 3.89 (s, 3H), 3.80 (s, 3H), 3.38 (ddd, $J=19.4, 12.7, 5.6$ Hz, 2H), 2.23 (s, 3H). ¹³C NMR (100 MHz, CDCl₃) δ 167.6, 149.9, 149.6, 147.2, 144.5, 134.6, 128.4, 127.1, 122.4, 120.4, 118.5, 116.0, 113.7, 110.1, 108.5, 72.1, 68.3, 55.8, 51.7, 46.5, 13.5. HRMS (ESI+) m/z Calcd for C₂₁H₂₄ClNO₅Na [M+Na]⁺ 428.12352; Found 428.12292.

Methyl(E)-3-(4-(3-(3,4-difluorophenyl)

amino)-2-hydroxypropoxy)-3-methoxyphenyl)acrylate (D22)

Yield 71%; White solid; m.p. 87–89 °C. ¹H NMR (400 MHz, CDCl₃) δ 7.63 (d, $J=16.0$ Hz, 1H), 7.12–7.04 (m, 2H), 6.93 (ddd, $J=30.9, 16.0, 8.6$ Hz, 2H), 6.46 (ddd, $J=12.7, 6.7, 2.8$ Hz, 1H), 6.38–6.27 (m, 2H), 4.30–4.22 (m, 1H), 4.11 (ddd, $J=15.9, 9.6, 5.0$ Hz, 2H), 3.90 (s, 3H), 3.80 (s, 3H), 3.30 (ddd, $J=19.1, 12.7, 5.4$ Hz, 2H). ¹³C NMR (100 MHz, CDCl₃) δ 167.6, 150.9 (d, $J=245.0$ Hz), 149.8, 149.5, 145.2 (dd, $J=8.5, 2.0$ Hz), 144.5, 143.2 (d, $J=249.9$ Hz), 128.4, 122.4, 117.4 (dd, $J=18.0, 1.7$ Hz), 116.1, 113.5, 110.1, 108.4 (dd, $J=5.5, 3.1$ Hz), 101.8 (d, $J=20.8$ Hz), 72.0, 68.3, 55.8, 51.7, 46.9. ¹⁹F NMR (376 MHz, CDCl₃) δ -137.12, -152.50. HRMS (ESI+) m/z Calcd for C₂₀H₂₁F₂NO₅Na [M+Na]⁺ 416.12800; Found 416.12744.

Methyl(E)-3-(4-(3-(4-chloro-2-methylphenyl)

amino)-2-hydroxypropoxy)-3-methoxyphenyl)acrylate (D23)

Yield 81%; White solid; m.p. 99–101 °C. ¹H NMR (400 MHz, CDCl₃) δ 7.62 (d, $J=15.9$ Hz, 1H), 7.13–6.98 (m, 4H), 6.87 (d, $J=8.3$ Hz, 1H), 6.55 (d, $J=8.5$ Hz, 1H), 6.32 (d, $J=15.9$ Hz, 1H), 4.31 (ddd, $J=10.7, 6.7, 4.2$ Hz, 1H), 4.11 (ddd, $J=16.1, 9.7, 5.1$ Hz, 2H), 3.87 (s, 3H), 3.80 (s, 3H), 3.35 (ddd, $J=19.5, 12.7, 5.6$ Hz, 2H), 2.12 (s, 3H). ¹³C NMR (100 MHz, CDCl₃) δ 167.6, 149.9, 149.6, 144.6, 144.5, 129.8, 128.3, 126.6, 124.4, 122.4, 122.0, 116.0, 113.6, 111.1, 110.2, 72.09, 68.4, 55.8, 51.7, 46.5, 17.3. HRMS (ESI+) m/z Calcd for C₂₁H₂₄ClNO₅K [M+K]⁺ 444.09746; Found 444.09735.

Methyl(E)-3-(4-(3-(3-chloro-4-fluorophenyl)

amino)-2-hydroxypropoxy)-3-methoxyphenyl)acrylate (D24)

Yield 93%; White solid; m.p. 123–125 °C. ¹H NMR (400 MHz, CDCl₃) δ 7.63 (d, $J=15.9$ Hz, 1H), 7.14–7.02 (m, 2H), 6.99–6.83 (m, 2H), 6.66 (dd, $J=6.1, 2.8$ Hz, 1H), 6.56–6.42 (m, 1H), 6.32 (d, $J=15.9$ Hz, 1H), 4.26 (dq, $J=6.3, 4.3$ Hz, 1H), 4.11 (ddd, $J=15.9, 9.6, 5.0$ Hz, 2H), 3.90 (s, 3H), 3.80 (s, 3H), 3.30 (ddd, $J=19.1, 12.6, 5.4$ Hz, 2H). ¹³C NMR (100 MHz, CDCl₃) δ 167.6, 151.1 (d, $J=238.2$ Hz), 149.8, 149.5, 145.1 (d, $J=2.1$ Hz), 144.5, 128.4, 122.4, 121.0 (d, $J=18.5$ Hz), 116.8 (d, $J=22.0$ Hz), 116.0, 114.2, 113.5, 112.6 (d, $J=6.3$ Hz), 110.1, 72.0, 68.2, 55.8, 51.7, 46.9. ¹⁹F NMR (376 MHz, CDCl₃) δ -130.63.

HRMS (ESI+) m/z Calcd for C₂₀H₂₁FCINO₅K [M+K]⁺ 448.07239; Found 448.07123.

Biological activity test method

In vitro antibacterial activity test

The turbidity method was used to evaluate the in vitro antibacterial activity of all target compounds against *Xoo* and *Xac* [15, 39]. Dimethyl sulfoxide (DMSO) was used as a negative control, and the commercial bactericides thiodiazole copper (TC) and bismethiazol (BT) were used as positive controls. Add 4 mL nutrient broth (NB) medium, 1 mL test compound or commercial bactericides (the final concentration of the solution is 100 and 50 μ g/mL), and 40 μ L *Xoo* or *Xac* bacterial solution into the 15 mL test tube. Test the EC₅₀ value of the target compounds when the concentration was 100, 50, 25, 12.5, 6.25 μ g/mL, respectively. Then incubated the above sample solution in a shaker (180 rpm, 28 \pm 1 °C) for about 24–48 h, until the negative control grew to the logarithmic phase. Measure the optical density at 595 nm (OD₅₉₅) with a microplate reader (turbidity correction value = OD_{Value of medium containing bacteria} - OD_{Medium value without bacteria}), and the calculation formula for the inhibition rate I was: $I = (C - T) / C \times 100\%$. C represented the corrected absorbance value of the untreated NB medium, and T represented the corrected absorbance value of the treated NB medium. Each experiment was tested for three times.

In vivo antibacterial activity test

The curative and protective activities in potted plants of compound D24 against rice bacterial leaf blight were determined by Schaad's method [40, 41]. Dimethyl sulfoxide (DMSO) was used as a negative control, and the commercial agricultural antibacterial agents thiodiazole copper (TC) and bismethiazol (BT) were used as positive controls. Under greenhouse control conditions, the curative activity of compound D24 against rice bacterial leaf blight was determined. Inoculate rice leaves with *Xoo* that has grown to the logarithmic growth stage. Rice leaves were inoculated with *Xoo* which had reached logarithmic growth stage. One day after inoculation, 200 μ g/mL of compound D24 solution was evenly sprayed on the rice leaves, and distilled water containing DMSO was evenly sprayed on the plants. Then they were placed in a plant growth room (28 °C and 90% RH) for 14 days to determine the disease index of rice leaves. Similarly, compound D24 had protective activity against rice bacterial leaf blight. 200 μ g/mL compound D24 solution was evenly sprayed on rice leaves, spray distilled water containing DMSO was evenly sprayed on the plants. One day

after spraying, the rice leaves were inoculated with *Xoo* that had grown to the logarithmic growth stage. Then they were placed in a plant growth room (28 °C and 90% RH) for 14 days to determine the disease index of rice leaves. The control efficiency of compound **D24**'s curative and protective activities $I (%) = (C - T)/C \times 100%$, where C was the disease index of the negative control group, and T was the disease index of the treatment group.

In vivo anti-TMV activity test

The inhibitory effect of the target compounds on TMV was tested by literature method [42]. Before the test, tobacco leaves with the same size, shape and age of left and right leaves were selected. The curative activity test was to wash and dry the tobacco 30 min after inoculation with TMV virus, and then apply the prepared target compound solution on the left side of the tobacco and the blank control solvent on the right side. The protective activity test was to smear the prepared target compound solution on the left side of tobacco leaves and the blank control solution on the right side of tobacco leaves, inoculate TMV virus after 20–22 h, wash it with clean water after 30 min, and then dry it naturally. The inactivation activity was to evenly mix the same volume of virus solution with the drug solution of the target compound for 30 min and then apply it on the left side of the tobacco leaf, apply the mixed solution of equal volume of virus solution and blank solvent on the right side of the tobacco leaf as the control, and rinse it with clean water after 30 min. The activity of the compounds was calculated using the following formula. Inhibition rate $I (%) = (C_{av} - T_{av})/C_{av} \times 100%$, where C is the number of lesions in leaves without compound treatment, T is the number of lesions in leaves treated with compound, and av is the average of the number of lesions.

Results and discussion

Antibacterial activity in vitro screening of target compounds

On the basis of previous work, the antibacterial activity of the target compounds was tested by turbidity method [15, 16, 39]. The preliminary results of the in vitro antibacterial activities of target compounds **D1–D24** against *Xoo* and *Xac* are shown in Table 1. Some compounds showed moderate antibacterial activity. Compound **D24** showed good inhibitory activity against *Xoo* (90.7% and 80.6% at concentrations of 100 and 50 µg/mL, respectively), similar to **BT** (90.1% and 80.2%, respectively). The antibacterial activity of compounds **D3**, **D5**, **D7**, **D22**, and **D23** against *Xoo* was higher than that of **TC** (65.7% and 46.9% at concentrations of 100 and 50 µg/

Table 1 In vitro antibacterial activity of the target compounds against *Xoo* and *Xac*

Compd	<i>Xoo</i>		<i>Xac</i>	
	Inhibition rate (%)		Inhibition rate (%)	
	100 µg/mL	50 µg/mL	100 µg/mL	50 µg/mL
D1	26.5 ± 1.9	21.8 ± 1.2	47.4 ± 1.9	32.1 ± 1.8
D2	35.6 ± 2.1	31.8 ± 3.8	55.3 ± 0.5	45.9 ± 3.3
D3	77.8 ± 2.8	66.4 ± 2.7	68.2 ± 2.7	48.7 ± 1.9
D4	28.2 ± 2.7	28.0 ± 1.1	25.2 ± 0.2	15.7 ± 2.6
D5	72.0 ± 1.3	55.0 ± 1.2	22.5 ± 3.7	21.4 ± 0.9
D6	35.2 ± 0.9	17.1 ± 3.0	29.7 ± 4.5	22.4 ± 4.7
D7	66.5 ± 1.8	47.9 ± 1.0	74.5 ± 2.3	60.0 ± 2.5
D8	25.3 ± 1.8	19.9 ± 2.2	31.9 ± 3.5	27.8 ± 2.6
D9	47.4 ± 1.3	32.8 ± 2.9	36.2 ± 2.2	12.0 ± 4.8
D10	26.8 ± 3.6	23.6 ± 2.7	33.1 ± 2.6	29.9 ± 0.1
D11	33.0 ± 1.2	32.4 ± 3.6	68.5 ± 3.5	45.3 ± 1.8
D12	22.7 ± 1.8	22.6 ± 3.7	33.5 ± 1.0	33.0 ± 0.7
D13	34.5 ± 2.4	26.8 ± 1.3	28.6 ± 1.9	15.4 ± 3.1
D14	36.7 ± 4.4	22.9 ± 1.1	26.7 ± 4.0	12.6 ± 3.3
D15	43.4 ± 2.9	26.4 ± 4.0	57.9 ± 3.2	45.9 ± 1.9
D16	42.2 ± 0.6	26.4 ± 3.1	31.1 ± 3.9	19.8 ± 4.2
D17	20.6 ± 1.8	8.7 ± 2.8	28.2 ± 3.8	12.8 ± 2.6
D18	32.9 ± 2.1	30.0 ± 0.8	27.7 ± 4.1	26.3 ± 2.4
D19	24.9 ± 3.5	19.8 ± 2.0	25.1 ± 1.3	14.2 ± 4.3
D20	34.2 ± 0.6	5.2 ± 2.2	34.4 ± 1.6	20.9 ± 0.1
D21	38.6 ± 2.6	37.7 ± 1.8	26.0 ± 3.0	21.6 ± 3.0
D22	89.1 ± 3.7	68.0 ± 3.1	35.7 ± 3.5	24.7 ± 2.5
D23	79.9 ± 1.0	63.6 ± 3.6	28.5 ± 2.2	23.1 ± 3.5
D24	90.7 ± 0.8	80.6 ± 2.7	25.9 ± 1.8	21.7 ± 3.7
BT^a	90.1 ± 2.3	80.2 ± 1.3	64.6 ± 1.9	51.2 ± 1.4
TC^a	65.7 ± 0.9	46.9 ± 2.6	76.8 ± 0.7	65.2 ± 2.0

Average of three replicates

^a The commercial agricultural antibacterial agents bismethiazol (BT) and thiodiazole copper (TC) were used as positive control

mL, respectively). Compounds **D2**, **D3**, **D7**, **D11**, and **D15** had moderate antibacterial activity against *Xac* at 100 µg/mL, with the inhibitory activity of compounds **D3**, **D7** and **D11** slightly higher than that of **BT** (which was 64.6%). To further quantify the antibacterial activity, the concentration values for 50% of maximal effect (EC_{50}) were determined for select compounds (Table 2). The EC_{50} values of compounds **D22** and **D24** on *Xoo* were 14.5 and 16.2 µg/mL, respectively, which were better than that of **TC** (44.5 µg/mL) and similar to that of **BT** (16.2 µg/mL). Compounds **D3**, **D7** and **D11** had inhibitory effects on *Xac*, and their EC_{50} values (37.3, 29.4 and 45.6 µg/mL, respectively) were slightly better than the EC_{50} of **BT** (46.8 µg/mL).

Table 2 Antibacterial activities of some target compounds against *Xoo* and *Xac* in vitro

Compd	<i>Xoo</i>			<i>Xac</i>		
	Regression equation	R ²	EC ₅₀ (μg/mL)	Regression equation	R ²	EC ₅₀ (μg/mL)
D1				y = 0.54x + 3.8	0.94	122.9 ± 4.9
D2				y = 0.78x + 3.5	0.97	74.2 ± 3.9
D3	y = 0.84x + 3.9	0.99	20.3 ± 0.9	y = 0.92x + 3.5	0.96	37.3 ± 1.4
D5	y = 0.87x + 3.7	0.93	27.1 ± 2.5			
D7	y = 1.16x + 3.0	0.98	45.4 ± 1.3	y = 1.13x + 3.3	0.99	29.4 ± 4.1
D11				y = 0.99x + 3.3	0.93	45.6 ± 0.5
D15				y = 0.99x + 3.3	0.96	66.1 ± 4.7
D22	y = 1.33x + 3.3	0.95	16.2 ± 1.5			
D23	y = 1.02x + 3.6	0.94	19.5 ± 0.6			
D24	y = 1.46x + 3.2	0.95	14.5 ± 0.8			
BT ^a	y = 1.62x + 3.0	0.98	16.2 ± 3.4	y = 0.83x + 3.6	0.95	46.8 ± 5.0
TC ^a	y = 0.93x + 3.4	0.97	44.5 ± 3.4	y = 1.04x + 3.5	0.95	23.8 ± 4.9

Average of three replicates

^a The commercial agricultural antibacterial agents bismethiazol (BT) and thiodiazole copper (TC) were used as positive control**Table 3** The protective activity of compound D24 against *Xanthomonas oryzae* pv. *oryzae* in vivo at 200 μg/mL

Treatment	14 days after spraying		
	Morbidity (%)	Disease Index (%)	Control efficiency (%) ^a
D24	100	42.2D	50.1A
BT ^b	100	45.8C	45.8B
TC ^b	100	47.6B	43.7C
CK ^c	100	84.6A	

^a Statistical analysis was conducted by the analysis of variance method under the conditions of equal variances assumed ($P > 0.05$) and equal variances not assumed ($P < 0.05$). Different uppercase letters indicate the values of protection activity with significant difference among different treatment groups at $P < 0.05$ ^b Commercial bactericides bismethiazol (BT) and thiodiazole copper (TC) were used as positive control agents^c Negative control

Antibacterial activity in vivo

Based on its promising antibacterial activity in vitro, the in vivo activity of compound D24 against rice bacterial leaf blight at 200 μg/mL was determined, and the results are shown in Tables 3 and 4, and Fig. 3. The protective activity of D24 was 50.1%, higher than that of BT (45.8%) and TC (43.7%). Compound D24 also had good curative activity (50.5%), superior to that of BT (47.1%) and TC (46.1%).

Anti-TMV activity in vivo screening of target compounds

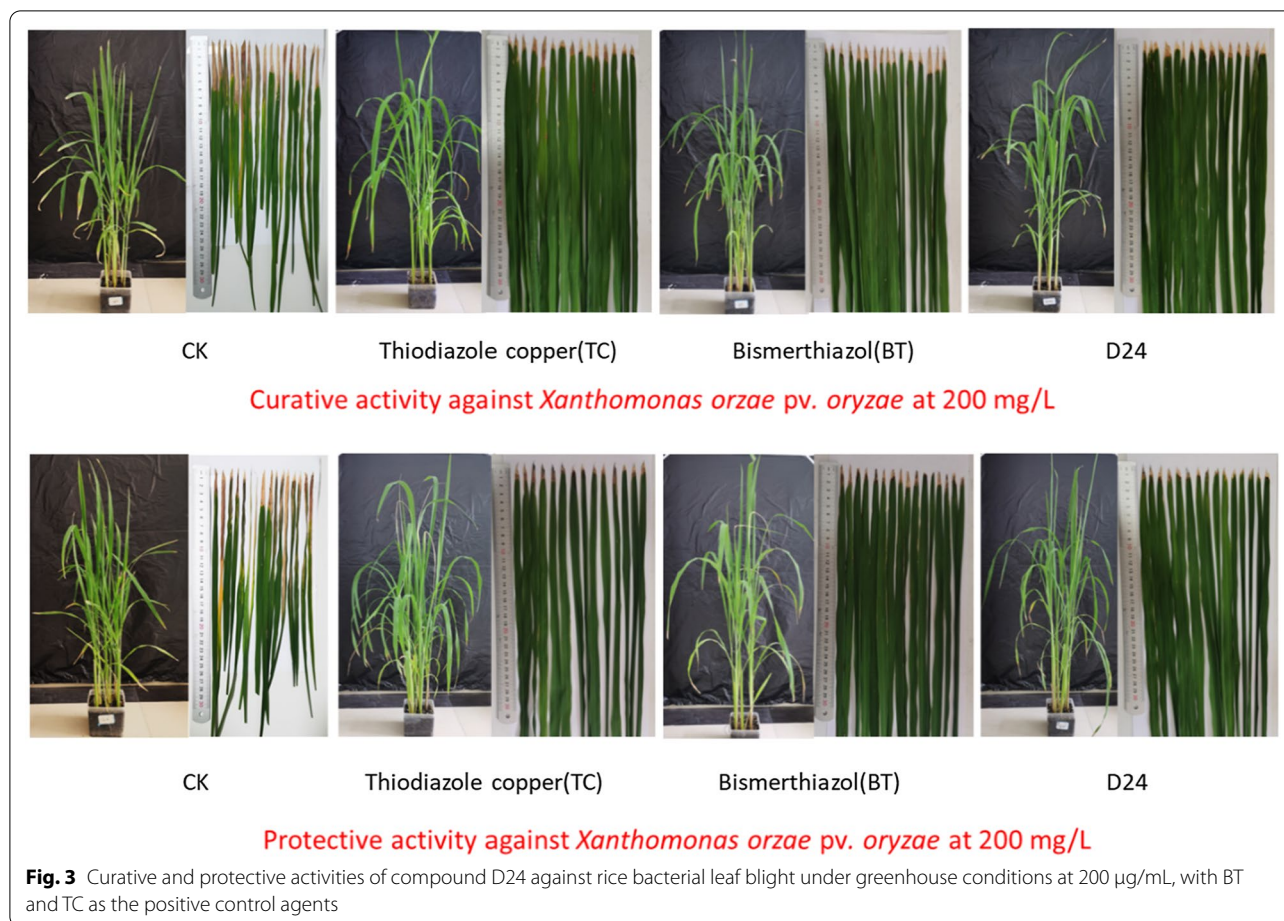
The inhibitory effect of ferulic acid derivatives D1–D24 on TMV was further studied based on the method of literature and the previous work of antiviral activity test

Table 4 The curative activity of compound D24 against *Xanthomonas oryzae* pv. *oryzae* in vivo at 200 μg/mL

Treatment	14 days after spraying		
	Morbidity (%)	Disease Index (%)	Control efficiency (%) ^a
D24	100	42.8C	50.5A
BT ^b	100	45.8B	47.1B
TC ^b	100	46.6B	46.1C
CK ^c	100	86.7A	

^a Statistical analysis was conducted by the analysis of variance method under the conditions of equal variances assumed ($P > 0.05$) and equal variances not assumed ($P < 0.05$). Different uppercase letters indicate the values of protection activity with significant difference among different treatment groups at $P < 0.05$ ^b Commercial bactericides bismethiazol (BT) and thiodiazole copper (TC) were used as positive control agents^c Negative control

[1, 12, 42]. The bioassay results indicated that most of the compounds exhibited moderate to good anti-TMV activity at 500 μg/mL, as shown in Table 5. The curative activities of compounds D1, D5, D12, D13, D18, D21, and D24 were 56.1, 59.3, 59.8, 53.9, 45.5, 74.0, and 74.1%, respectively, which were better than that of ribavirin (44.8%). Compounds D21 and D24 (74.0 and 74.1%, respectively) showed slightly higher curative activity than ningnanmycin (70.0%). Compounds D3, D4, D5, D7, D9, D14, D18, D20, and D24 exhibited good protective activity (respectively 54.6, 52.6, 59.6, 53.1, 70.7, 74.3, 68.1, 51.9, and 54.9%), higher than ribavirin (50.0%). Compounds D9, D14 and D18 (70.7, 74.3 and 68.1%, respectively) showed better activity



than ningnanmycin (65.3%). Most of the compounds showed excellent inactivation activity against TMV compared to ribavirin (73.5%). Notably, compound **D3** (93.7%) was slightly better than ningnanmycin (93.2%). The EC_{50} values of the inactivation activity of some compounds were tested, and the results are shown in Table 6. In particular, the EC_{50} value of compound **D3** was 38.1 $\mu\text{g}/\text{mL}$, which was higher than that of ningnanmycin ($\text{EC}_{50} = 39.2 \mu\text{g}/\text{mL}$).

Autodocking and MD simulation

Based on previous work [43, 44], the interaction between the active target compounds and TMV coat protein (TMV-CP) (PDB 97 code: 1EI7) was investigated. The binding mode of compound **D3** and TMV-CP was studied by molecular docking, and the results are shown in Fig. 4. Compound **D3** has a strong affinity for TMV-CP with a binding energy of $-7.54 \text{ kcal}/\text{mol}$, which is better than that of ningnanmycin ($-6.88 \text{ kcal}/\text{mol}$). Binding to the active site of TMV-CP was achieved through amino acid residues that play a key role in the self-assembly of

TMV-CP, including GLY137, ASN73, THR136, VAL75, SER143 and VAL260 (Fig. 4A and B). Among them, there is a strong hydrogen bond interaction between compound **D3** and key residues (GLY137 and ASN73), the bond lengths of which are 3.1 Å and 2.9 Å, respectively, and GLY137 also interacts with ningnanmycin. The carbon atoms of compound **D3** and ningnanmycin interact with THR136 and VAL75 residues through hydrophobic bonds, and a halogen bond is formed between **D3** and SER143. Therefore, compound **D3** may be the same as ningnanmycin, disrupting the three-dimensional structure of TMV-CP, making TMV particles unable to self-assemble, thereby achieving antiviral effects.

Molecular dynamics (MD) simulations were used to evaluate the stability of compound **D3** and ningnanmycin. Under simulated conditions, the root-mean-square deviation (RMSD) of the atom from its initial position was measured and recorded (Fig. 4C and D). The interaction of other binding site residues affects the energy and geometric characteristics, so that the ligand obtains a stable conformation at the active site.

Table 5 Antiviral activities of target compounds against TMV in vivo at 500 µg/mL^a

Compd	Curative activity (%)	Protective activity (%)	Inactivation activity (%)
D1	56.1 ± 0.8	49.9 ± 3.9	76.9 ± 1.4
D2	31.8 ± 4.8	41.8 ± 3.5	89.1 ± 3.8
D3	37.5 ± 0.8	54.6 ± 2.5	93.7 ± 1.9
D4	38.8 ± 4.5	52.6 ± 4.5	89.5 ± 1.5
D5	59.3 ± 0.7	59.6 ± 4.9	72.9 ± 2.7
D6	25.1 ± 2.7	35.1 ± 0.1	73.0 ± 1.7
D7	31.8 ± 0.7	53.1 ± 0.5	74.2 ± 2.8
D8	40.9 ± 2.7	47.2 ± 0.8	85.2 ± 3.1
D9	31.5 ± 3.6	70.7 ± 5.0	84.9 ± 1.9
D10	38.4 ± 3.3	31.4 ± 1.1	84.3 ± 4.9
D11	35.4 ± 1.0	34.2 ± 0.1	74.1 ± 2.0
D12	59.8 ± 1.3	39.9 ± 1.1	61.2 ± 0.3
D13	53.9 ± 4.7	39.8 ± 4.9	71.4 ± 0.4
D14	21.8 ± 4.5	74.3 ± 3.7	81.2 ± 2.5
D15	32.3 ± 4.5	35.0 ± 2.4	82.7 ± 3.3
D16	22.5 ± 4.8	19.0 ± 3.7	84.9 ± 3.4
D17	33.6 ± 2.5	43.9 ± 2.2	82.5 ± 3.6
D18	45.5 ± 3.2	68.1 ± 3.3	84.1 ± 4.5
D19	34.6 ± 2.1	43.7 ± 3.6	85.6 ± 4.2
D20	42.8 ± 0.1	51.9 ± 1.6	81.8 ± 0.7
D21	74.0 ± 4.0	41.5 ± 2.1	60.1 ± 0.1
D22	20.2 ± 1.7	43.6 ± 2.5	66.8 ± 0.7
D23	40.2 ± 3.6	54.9 ± 2.7	74.5 ± 1.5
D24	74.1 ± 1.9	47.4 ± 2.6	74.2 ± 0.8
Ribavirin	44.8 ± 1.2	50.0 ± 1.8	73.5 ± 1.6
Ningnanmycin	70.0 ± 3.8	65.3 ± 2.5	93.2 ± 0.5

^a All active values are the average of three duplicates**Table 6** EC₅₀ of some target compounds anti-TMV activity

Compd	Regression equation	R ²	EC ₅₀ of inactivation activity ^a
D2	y = 1.33x + 2.6	0.99	56.8 ± 4.4
D3	y = 1.26x + 3.0	0.96	38.1 ± 1.4
D4	y = 1.29x + 2.7	0.98	52.5 ± 4.4
D8	y = 1.15x + 2.9	0.99	57.3 ± 2.9
D19	y = 1.12x + 3.0	0.99	57.9 ± 4.0
Ningnanmycin ^b	y = 1.37x + 2.8	0.99	39.2 ± 3.8

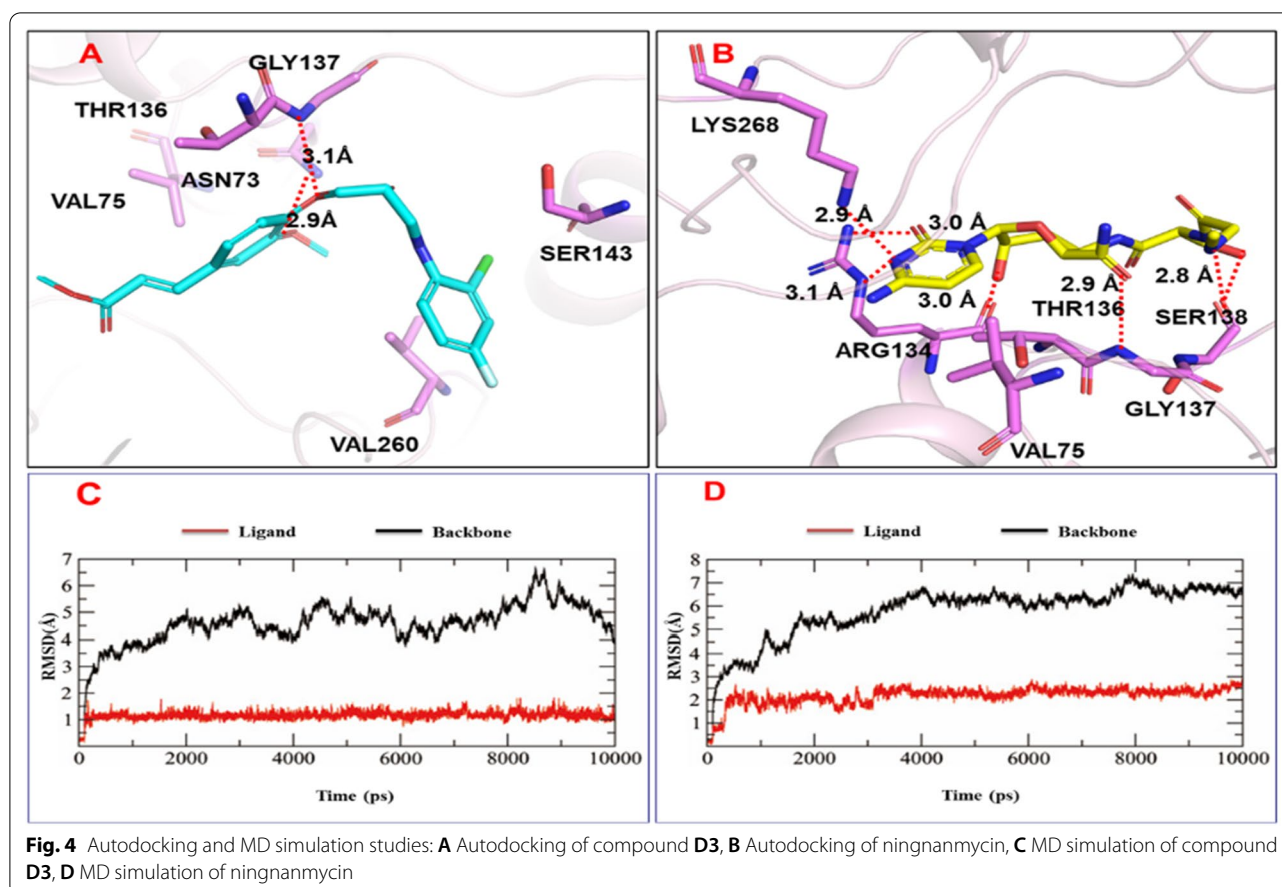
^a Average of three replicates^b Ningnanmycin was used as the control

Structure–activity relationship analysis

The preliminary structure–activity relationship (SAR) indicated that different substituents of ferulic acid compounds had a strong influence on their activity against

Xoo, *Xac* and TMV. According to Table 1, the position and number of substituted fluorine atoms on the aromatic ring had a significant effect on the inhibition of *Xoo*. When the substituents are two fluorine atoms at the same time, the activity of the compounds towards *Xoo* is different: **D22** (R = 3,4-di-F-Ph) > **D14** (R = 3,5-di-F-Ph) > **D2** (R = 2,4-di-F-Ph). The introduction of chlorine atoms to the electron-withdrawing group improved the activity of the compound: **D24** (R = 3-Cl-4-F-Ph) and **D3** (R = 2-Cl-4-F-Ph) > **D13** (R = 3-CH₃-4-F-Ph) and **D1** (R = 2-CH₃-4-F-Ph). Compounds with weak electron-withdrawing effects at the same position had higher activity: **D23** (R = 4-Cl-2-CH₃-Ph), **D18** (R = 4-Br-2-CH₃-Ph) > **D1** (R = 4-F-2-CH₃-Ph). The introduction of substituents on the benzene ring helps to improve the antibacterial activity against *Xac*: **D7** (R = 4-Cl-3-F-Ph) > **D11** (R = 3-NO₂-4-F-Ph) > **D3** (R = 2-CH₃-5-F-Ph) > **D15** (R = 5-CH₃-2-F-Ph) > **D2** (R = 2,4-di-F-Ph) > **D1** (R = 2-CH₃-4-F-Ph) > **D5** (R = Ph). Different halogens and positions influenced the activity of the compound: **D7** (R = 4-Cl-3-F-Ph) > **D9** (R = 4-Br-3-F-Ph), **D3** (R = 2-Cl-4-F-Ph) > **D24** (R = 3-Cl-4-F-Ph).

According to Table 5, increasing the number of fluorine atoms increased the curative activity against TMV, particularly in the case of 2,4 substituted difluoride: **D8** (R = 2,4,5-tri-F-Ph) > **D2** (R = 2,4-di-F-Ph) > **D14** (R = 3,5-di-F-Ph), **D22** (R = 3,4-di-F-Ph). The electron-withdrawing at the same position is more active than the electron-donating, and the compound with a strong electron-withdrawing effect were more active: **D1** (R = 4-F-2-CH₃-Ph) > **D18** (R = 4-Br-2-CH₃-Ph), **D23** (R = 4-Cl-2-CH₃-Ph) > **D10** (R = 4-OCH₃-2-CH₃-Ph). The protective activity sequence of compounds with two electron-withdrawing substituents on the benzene ring was as follows: **D14** (R = 3,5-di-F-Ph) > **D9** (R = 4-Br-3-F-Ph) > **D3** (R = 2-Cl-4-F-Ph) > **D7** (R = 4-Cl-3-F-Ph) > **D20** (R = 4-I-2-F-Ph) > **D24** (R = 3-Cl-4-F-Ph) > **D22** (R = 3,4-di-F-Ph) > **D2** (R = 2,4-di-F-Ph) > **D6** (R = 4-F-3-CF₃-Ph) > **D11** (R = 3-NO₂-4-F-Ph). The electron-donating group on the benzene ring can improve the inactivation activity of the compound: **D19** (R = 3,4-di-OCH₃-Ph) > **D10** (R = 4-OCH₃-2-CH₃-Ph) > **D17** (R = 4-CH(CH₃)₂-Ph) > **D5** (R = Ph). The same halogen introduced at different positions had different activities: **D4** (R = 5-F-2-CH₃-Ph) > **D1** (R = 4-F-2-CH₃-Ph), **D23** (R = 4-Cl-2-CH₃-Ph) > **D21** (R = 3-Cl-2-CH₃-Ph). In general, the R substituents of the compounds resulting in better anti-TMV activity or inhibition of *Xoo* and *Xac* frequently contained fluorine atoms. The introduction of fluorine atoms into compounds is known to effectively alter conformation, membrane permeability, lipophilicity, metabolic pathways, and pharmacokinetic properties, and can improve biological activity in many



cases [45, 46]. However, it is also affected by other factors such as the position of the substituent and the influence of other substituents on the fluorine atom, which leads to changes in the activity of the compound.

Conclusion

In summary, a series of ferulic acid derivatives containing an β -amino alcohol were designed and synthesized, and the biological activities of the target compounds were evaluated. Bioassays results showed that compound **D24** had a good inhibitory effect on *Xoo*, which was superior to the commercial bactericide **BT** and **TC**. The inhibitory effect of compound **D7** on *Xac* was also higher than **BT** and close to **TC**. As compound **D3** ($EC_{50} = 39.2 \mu\text{g/mL}$) had good passivating activity against TMV, the interaction of the ligand molecules with TMV-CP was explored by molecular docking and molecular dynamics simulations. The results of molecular docking indicated that compound **D3** was inserted into the active site of TMV-CP through amino acid residues, and had a strong affinity for TMV-CP with a binding energy of -7.54 kcal/mol , which was superior to the commercial antiviral agent

ningnanmycin (-6.88 kcal/mol). Therefore, the three-dimensional structure of the TMV coat protein may be disrupted by the compounds **D3** and ningnanmycin, preventing the TMV particles from self-assembling and thus producing a potent antiviral effect. The synthetic compounds in this work may provide potential lead compounds for the discovery of novel plant fungicides and antivirals.

Abbreviations

Xoo: *Xanthomonas oryzae* Pv. *oryzae*; *Xac*: *Xanthomonas axonopodis* Pv. *citri*; TMV: Tobacco mosaic virus; FA: Ferulic acid; TC: Thiodiazole copper; BT: Bismethiazol; $^1\text{H NMR}$: ^1H nuclear magnetic resonance; $^{13}\text{C NMR}$: ^{13}C nuclear magnetic resonance; $^{19}\text{F NMR}$: ^{19}F nuclear magnetic resonance; HRMS: High-resolution mass spectrum.

Supplementary Information

The online version contains supplementary material available at <https://doi.org/10.1186/s13065-022-00828-8>.

Additional file 1. $^1\text{H NMR}$, $^{13}\text{C NMR}$, $^{19}\text{F NMR}$, and HR-MS spectra of the title compounds D1–D24.

Acknowledgements

The authors express their sincere thanks to Prof. Gefei Hao for his guidance on docking study, and Prof. Xiangyang Li for providing the microorganisms of *Xoo*, *Xac*, and TMV.

Author contributions

Synthesis: AD; Bio-assay: AD and LY; Data curation: AD, LY, ZZ; Computational chemistry and the analysis of docking: YH; Writing—original draft: AD; Project administration: JW; Writing—review and editing: AD, ZZ and JW. All authors read and approved the final manuscript.

Funding

The Natural Science Foundation of China (NSFC) (Nos. 32072445 and 21762012), the S&T Planning Project of Guizhou Province (Nos. [2017] 1402 and [2017] 5788), the Program of Introducing Talents to Chinese Universities (111 Program, D20023), and the Natural Science Research Project of Guizhou Education Department (KY[2018]009).

Availability of data and materials

All data generated or analyzed during this study are included in this published article (and its Additional file 1).

Declarations

Ethics approval and consent to participate

In this study, all the experimental research on plants were conducted under the guidelines set by the Institutional Bioethics Committee, Guizhou University. All the plants (tobacco and rice) were cultivated in our green house. The *Xoo*, *Xac* were isolated from the rice plant, tobacco mosaic virus (TMV) was isolated from the tobacco plant, all the plants were growth in the field without uprooting. For our studied purpose, permission was granted by the owner of the field. These microorganisms were identified and preserved by Prof. Xiangyang Li in our laboratory.

Consent for publication

Not applicable.

Competing interests

The authors declare that they have no competing interests.

Received: 22 January 2022 Accepted: 6 May 2022

Published online: 17 May 2022

References

- Guo SX, Zhao W, Wang YY, Zhang W, Chen SH, Wei PP, Wu J. Design, synthesis, and mechanism of antiviral acylurea derivatives containing a trifluoromethylpyridine moiety. *J Agric Food Chem*. 2021;69:12891–9.
- Huang GY, Cui C, Wang ZP, Li YQ, Xiong LX, Wang LZ, Yu SJ, Li ZM, Zhao WG. Synthesis and characteristics of (hydrogenated) ferulic acid derivatives as potential antiviral agents with insecticidal activity. *Chem Cent J*. 2013;7:33.
- Wu ZX, Zhang J, Chen JX, Pan JK, Zhao L, Liu DY, Zhang AW, Chen J, Hu DY, Song BA. Design, synthesis, antiviral bioactivity and three-dimensional quantitative structure–activity relationship study of novel ferulic acid ester derivatives containing quinazoline moiety. *Pest Manag Sci*. 2017;73:2079–89.
- Tang X, Zhang C, Chen M, Xue YN, Liu TT, Xue W. Synthesis and antiviral activity of novel myricetin derivatives containing a ferulic acid mmide scaffolds. *New J Chem*. 2020;44:2374–9.
- Tao H, Tian H, Jiang S, Xiang XW, Lin YN, Ahmeda W, Tang RY, Cui ZN. Synthesis and biological evaluation of 1,3,4-thiadiazole derivatives as type III secretion system inhibitors against *Xanthomonas oryzae*. *Pestic Biochem Physiol*. 2019;160:87–94.
- Chen JX, Luo YQ, Wei CL, Wu SK, Wu R, Wang SB, Hu DY, Song BA. Novel sulfone derivatives containing a 1,3,4-oxadiazole moiety: design and synthesis based on the 3D-QSAR model as potential antibacterial agent. *Pest Manag Sci*. 2020;76:3188–98.
- Jadhav RR, Apet KT, Kadam DS. Investigations on role of stomata in development of citrus canker caused by *Xanthomonas axonopodis* pv. *Citri*. *Int J Curr Microbiol Appl Sci*. 2020;9:3497–506.
- Dan WJ, Tuong TML, Wang DC, Li D, Zhang AL, Gao JM. Natural products as sources of new fungicides (V): design and synthesis of acetophenone derivatives against phytopathogenic fungi *in vitro* and *in vivo*. *Bioorg Med Chem Lett*. 2018;28:2861–4.
- Lan XM, Xie DD, Yin LM, Wang ZZ, Chen J, Zhang AW, Song A, Hu DY. Novel α , β -unsaturated amide derivatives bearing α -amino phosphonate moiety as potential antiviral agents. *Bioorg Med Chem Lett*. 2017;27:4270–3.
- Dulong V, Kouassi MC, Labat B, Cerf DL, Picton L. Antioxidant properties and bioactivity of carboxymethylpullulan grafted with ferulic acid and of their hydrogels obtained by enzymatic reaction. *Food Chem*. 2018;262:21–9.
- Wu M, Wang ZW, Meng CS, Wang KL, Hu YN, Wang LZ, Wang QM. Discovery and SARs of trans-3-aryl acrylic acids and their analogs as novel anti-tobacco mosaic virus (TMV) agents. *PLoS ONE*. 2013;8:e56475.
- He F, Wei PP, Yu G, Guo SX, Zheng ZG, Chen SH, Dai AL, Zhang RF, Wu ZX, Wu J. Synthesis of trans-methyl ferulate bearing an oxadiazole ether as potential activators for controlling plant virus. *Bioorg Chem*. 2021;115:105248.
- Wang ZZ, Xie DD, Gan XH, Zeng S, Zhang AW, Yin LM, Song BA, Jin LH, Hu DY. Synthesis, antiviral activity, and molecular docking study of trans-ferulic acid derivatives containing acylhydrazone moiety. *Bioorg Med Chem Lett*. 2017;27:4096–100.
- Wang KL, Hu YN, Liu YX, Mi N, Fan ZJ, Liu Y, Wang QM. Design, synthesis, and antiviral evaluation of phenanthrene-based tylophorine derivatives as potential antiviral agents. *J Agric Food Chem*. 2010;58:12337–42.
- Zhang RF, Deng P, Dai AL, Guo SX, Wang Y, Wei PP, Wu J. Design, synthesis, and biological activity of novel ferulic amide Ac5c derivatives. *ACS Omega*. 2021;6:27561–7.
- Zhang RF, Guo SX, Deng P, Wang Y, Dai AL, Wu J. Novel ferulic amide Ac6c derivatives: design, synthesis, and their antipest activity. *J Agric Food Chem*. 2021;69:10082–92.
- Khatkar A, Nanda A, Kumar P, Narasimhan B. Synthesis and antimicrobial evaluation of ferulic acid derivatives. *Res Chem Intermed*. 2015;41:299–309.
- Khatkar A, Nanda A, Kumar P, Narasimhan B. Purification and identification of active antibacterial components in *Carpobrotus edulis* L. *J Ethnopharmacol*. 2001;76:87–91.
- Kim HY, Park J, Lee KH, Lee DU, Kwak JH, Kim YS, Lee SM. Ferulic acid protects against carbon tetrachloride-induced liver injury in mice. *Toxicology*. 2011;282:104–11.
- Sgarbossa A, Giacomazza D, Carlo MD. Ferulic acid: a hope for alzheimer's disease therapy from plants. *Nutrients*. 2015;7:5764–82.
- Fang L, Kraus B, Lehmann J, Heilmann J, Zhang YH, Decker M. Design and synthesis of tacrine-ferulic acid hybrids as multi-potent anti-Alzheimer drug candidates. *Bioorg Med Chem Lett*. 2008;18:2905–9.
- Sergent T, Piront N, Meurice J, Toussaint O, Schneider YJ. Anti-inflammatory effects of dietary phenolic compounds in an *in vitro* model of inflamed human intestinal epithelium. *Chem-Biol Interact*. 2010;188:659–67.
- Li WX, Li NG, Tang YP, Li BQ, Liu L, Hang X, Fu HA, Duan JA. Biological activity evaluation and structure–activity relationships analysis of ferulic acid and caffeic acid derivatives for anticancer. *Bioorg Med Chem Lett*. 2012;22:6085–8.
- Fong Y, Tang CC, Hu HT, Fang HY, Chen BH, Wu CY, Yuan SS, Wang HMD, Chen YC, Teng YN, Chiu CC. Inhibitory effect of trans-ferulic acid on proliferation and migration of human lung cancer cells accompanied with increased endogenous reactive oxygen species and β -catenin instability. *Chin Med (London U K)*. 2016;11:45/1–45/13.
- Zhong YW, Dong YZ, Fang K, Izumi KJ, Xu MH, Lin GQ. A highly efficient and direct approach for synthesis of enantiopure β -aminoalcohols by reductive cross-coupling of chiral N-tert-butanesulfonyl imines with aldehydes. *J Am Chem Soc*. 2005;127:11956–7.
- Azizi N, Saidi MR. Highly chemoselective addition of amines to epoxides in water. *Org Lett*. 2005;7:3649–51.
- Testaa ML, Zaballosb E, Zaragoza RJ. Reactivity of β -amino alcohols against dialkyl oxalate: synthesis and mechanism study in the formation

- of substituted oxalamide and/or morpholine-2,3-dione derivatives. *Tetrahedron*. 2012;68:9583–91.
28. Ager DJ, Prakash I, Schaad DR. 1,2-amino alcohols and their heterocyclic derivatives as chiral auxiliaries in asymmetric synthesis. *Chem Rev*. 1996;96:835–76.
 29. Brien PO. Sharpless asymmetric aminohydroxylation: scope, limitations, and use in synthesis. *Angew Chem Int Ed*. 1999;38:326–9.
 30. Ferrarini SR, Duarte MO, Rosa RGD, Rolim V, Rolim GV, Ribeiro VLS. Acaricidal activity of limonene, limonene oxide and β -amino alcohol derivatives on *Rhipicephalus (Boophilus) microplus*. *Vet Parasitol*. 2008;157:149–53.
 31. Mejdrova I, Chalupska D, Plackova P, Muller C, Sala M, Klima M, et al. Rational design of novel highly potent and selective phosphatidylinositol 4-kinase III β (PI4KB) inhibitors as broad-spectrum antiviral agents and tools for chemical biology. *J Med Chem*. 2017;60:100–18.
 32. Agnieszka TK, Renata K, Marcin K, Bartosz S, Magdalena W, Patrycja G. Synthesis, absolute configuration, antibacterial, and antifungal activities of novel benzofuryl β -amino alcohols. *Materials*. 2020;13:4080.
 33. Wang PY, Xiang M, Luo M, Liu HW, Zhou X, Wu ZB, Liu LW, Li Z, Yang S. Novel piperazine-tailored ursolic acid hybrids as significant antibacterial agents targeting phytopathogens *Xanthomonas oryzae* pv. *oryzae* and *X. axonopodis* pv. *citri* probably directed by activation of apoptosis. *Pest Manage Sci*. 2020;76:2746–54.
 34. Zheng Y, Qiang X, Xu R, Song Q, Tian C, Liu H, Li W, Tan W, Deng Y. Synthesis and evaluation of pterostilbene β -amino alcohol derivatives as multifunctional agents for alzheimer's disease treatment. *Bioorg Chem*. 2018;78:298–306.
 35. Srivastava P, Vyas VK, Variya B, Patel P, Qureshi G, Ghate M. Synthesis, anti-inflammatory, analgesic, 5-lipoxygenase (5-LOX) inhibition activities, and molecular docking study of 7-substituted coumarin derivatives. *Bioorg Chem*. 2016;67:130–8.
 36. Vanguru S, Jilla L, Sajja Y, Bantu R, Nagarapu L, Nanubolu JB, Bhaskar B, Jain N, Sivan S, Manga V. A novel piperazine linked β -amino alcohols bearing a benzosuberone scaffolds as anti-proliferative agents. *Bioorg Med Chem Lett*. 2017;24:792–6.
 37. Baia B, Li XY, Li Y, Zhu HJ. Design, synthesis and cytotoxic activities of novel β -amino alcohol derivatives. *Bioorg Med Chem Lett*. 2011;21:2302–4.
 38. Xiang M, Song YL, Ji J, Zhou X, Liu LW, Wang PY, Wu ZB, Li Z, Yang S. Synthesis of novel 18 β -glycyrrheticin piperazine amides displaying significant *in vitro* and *in vivo* antibacterial activities against intractable plant bacterial diseases. *Pest Manage Sci*. 2020;76:2959–71.
 39. Yu G, Chen SH, Guo SX, Xu BX, Wu J. Trifluoromethylpyridine 1,3,4-oxadiazole derivatives: emerging scaffolds as bacterial agents. *ACS Omega*. 2021;6:31093–8.
 40. Wang PY, Zhou L, Zhou J, Wu ZB, Xue W, Song BA, Yang S. Synthesis and antibacterial activity of pyridinium-tailored 2,5-substituted-1,3,4-oxadiazole thioether/sulfoxide/ sulfonederivatives. *Bioorg Med Chem Lett*. 2016;26:1214–7.
 41. Zhu LZ, Zeng HN, Liu D, Fu Y, Wu Q, Song BA, Gan XH. Design, synthesis, and biological activity of novel 1,2,4-oxadiazole derivatives. *BMC Chem*. 2020;14:68.
 42. Wang YY, Xu FZ, Luo DX, Guo SX, He F, Dai AL, Song BA, Wu J. Synthesis of anthranilic diamide derivatives containing moieties of trifluoromethylpyridine and hydrazone as potential anti-viral agents for plants. *J Agric Food Chem*. 2019;67:13344–52.
 43. Luo DX, Guo SX, He F, Wang HY, Xu FZ, Dai AL, Zhang RF, Wu J. Novel anthranilic amide derivatives bearing the chiral thioether and trifluoromethylpyridine: synthesis and bioactivity. *Bioorg Med Chem Lett*. 2020;30: 126902.
 44. Luo DX, Guo SX, He F, Chen SH, Dai AL, Zhang RF, Wu J. Design, synthesis, and bioactivity of α -ketoamide derivatives bearing a vanillin skeleton for crop diseases. *J Agric Food Chem*. 2020;68:7226–34.
 45. Maienfisch P, Hall RG. The importance of fluorine in the life science industry. *Chimia*. 2004;58:93–9.
 46. Gillis EP, Eastman KJ, Hill MD, Donnelly DJ, Meanwell NA. Applications of fluorine in medicinal chemistry. *J Med Chem*. 2015;58:8315–59.

Publisher's Note

Springer Nature remains neutral with regard to jurisdictional claims in published maps and institutional affiliations.

Ready to submit your research? Choose BMC and benefit from:

- fast, convenient online submission
- thorough peer review by experienced researchers in your field
- rapid publication on acceptance
- support for research data, including large and complex data types
- gold Open Access which fosters wider collaboration and increased citations
- maximum visibility for your research: over 100M website views per year

At BMC, research is always in progress.

Learn more biomedcentral.com/submissions

